*M. Mostafaiyan[1,2] *, S. Wiessner[1,2], G. Heinrich[1,2]*

[1] *Leibniz-Institut für Polymerforschung Dresden e. V, Dresden, Germany*
[2] *Institut für Werkstoffwissenschaft, Technische Universität Dresden, Dresden, Germany*

Study of Dispersive and Distributive Mixing in a Converging Pipe

The creeping flow of a polymeric melt in a converging pipe is analyzed using an in-house finite element code. An introduced power-law model considers the shear thinning behavior of the viscous liquid. Furthermore, distributive and dispersive mixing processes are evaluated with the mean strain function and the Manas-Zloczower mixing index, respectively. Using a parametric study, the dependency of the mixing criteria on the rheological and geometrical factors is investigated. Finally, a new analytical expression for the evaluation of the distributive mixing is suggested, based on simplifying assumptions and a curve fitting method.

1 Introduction

Mixing is a crucial step in polymer processing, since all of the physical, mechanical and chemical properties are determined by the rearrangement and breakup of the minor or second phase, which are significantly influenced by the mixing process. The repeated rearrangement of the second phase determines the spatial homogeneity of the polymeric compound and is defined as the distributive mixing; and the break-up of second phase into smaller particles or droplets is categorized as dispersive mixing. Due to the importance of the mixing process, many researchers have studied distributive and dispersive mixing in different mixing and processing equipment, including single screw extruders (Alemaskin et al., 2005; Bigg and Middleman, 1974; Bigio et al., 1985; Erwin and Mokhtarian, 1983; Gale, 1997; Kwon et al., 1994; Wang et al., 2003) and twin screw extruders (Bigio and Zerafati, 1991; Galaktionov et al., 2002; Kalyon and Sangani, 1989; Li and Manas-Zloczower, 1995; Maheshri and Wyman, 1980; Wong and Manas-Zloczower, 1994) and internal mixers (Connelly and Kokini, 2004; Funt, 1977, Gogos and Tadmor, 1979; Manas-Zloczower, 2012; Yao and Manas-Zloczower, 1996).

Although, mixing process and morphology development are mainly carried out in the above mentioned mixing devices, the pressure flow in a die and its design can also have an important role in morphology development (Ausias et al., 1996). For example the design of the contraction and converging sections in a die can improve the dispersive mixing and the orientation of the second phase (Tokihisa et al., 2006). In this regard, some researchers have studied the microstructural features of mixing (Fard et al., 2008), such as second phase deformation in a pressure flow (Mostafaiyan et al., 2013; Zhou et al., 2008). Therefore, by considering the importance of the mixing in pressure flow, we have extended our previous research (Mostafaiyan et al., 2015) to study the dispersive mixing as well as the distributive mixing in the pressure flow in a converging pipe. This geometry has also many applications in the polymer processing field; namely, profile production and fiber spinning.

* Mail address: Mehdi Mostafaiyan, Leibniz-Institut für Polymerforschung Dresden e. V., Hohe Straße 6, D-01069 Dresden, Germany
E-mail: mostafaiyan@ipfdd.de, mehdi.mostafaiyan@gmail.com

2 Simulation Consideration

2.1 Governing Equations

In this section the principal equations for the calculation of the flow field of an incompressible polymeric melt in a converging or tapered pipe are introduced. Since polymeric flows are of low Reynolds number, it is possible to ignore inertial terms in equations of motion, and describe the flow by Stokes equations. Also, in cylindrical coordinates, according to the axisymmetric nature of the flow in the pipe, the swirl components of the fluid velocity as well as all derivations in the same direction are zero. Therefore, the equations of the creeping motion and the continuity in two-dimensional form can be expressed as follow:

$$\frac{1}{r}\frac{\partial}{\partial r}(r\tau_{rr}) + \frac{\partial \tau_{rz}}{\partial z} - \frac{\tau_{\theta\theta}}{r} = \frac{\partial P}{\partial r}, \tag{1a}$$

$$\frac{1}{r}\frac{\partial}{\partial r}(r\tau_{rz}) + \frac{\partial \tau_{zz}}{\partial z} = \frac{\partial P}{\partial z}, \tag{1b}$$

$$\frac{1}{r}\frac{\partial (rv)}{\partial r} + \frac{\partial u}{\partial z} = 0. \tag{1c}$$

In Eqs. 1a to 1c, u and v are velocities in the axis (z) and radial (r) directions, respectively; and P denotes pressure. The components of the stress tensor ($\bar{\bar{\tau}}$) are denoted with τ_{ij} (i,j = r,z). The stress tensor, for a generalized Newtonian fluid, is defined in Eq. 2 as follows:

$$\bar{\bar{\tau}} = -\eta \dot{\bar{\bar{\gamma}}}, \tag{2}$$

also, in Eq. 2, $\bar{\bar{\dot{\gamma}}}$ is the strain rate tensor, which is defined in Eq. 3:

$$\bar{\bar{\dot{\gamma}}} = \begin{pmatrix} 2\frac{\partial v}{\partial r} & 0 & \frac{\partial u}{\partial r}+\frac{\partial v}{\partial z} \\ 0 & 2\frac{v}{r} & 0 \\ \frac{\partial u}{\partial r}+\frac{\partial v}{\partial z} & 0 & 2\frac{\partial u}{\partial z} \end{pmatrix}, \tag{3}$$

moreover, in order to incorporate the shear thinning behavior of the polymeric melts, the viscosity term of η in Eq. 2 is described by power-law rules as follow:

$$\eta = k\dot{\gamma}^{n-1}. \tag{4}$$

In Eq. 4, k, n and $\dot{\gamma}$ are the consistency index, power-law index and magnitude of the strain rate tensor, respectively; the latest one is defined in Eqs. 5a and 5b:

$$\dot{\gamma} = \sqrt{\frac{1}{2}\bar{\bar{\dot{\gamma}}} : \bar{\bar{\dot{\gamma}}}} = \sqrt{\frac{1}{2}(\dot{\gamma}_{rr}^2 + \dot{\gamma}_{zz}^2 + \dot{\gamma}_{\theta\theta}^2 + \dot{\gamma}_{rz}^2 + \dot{\gamma}_{zr}^2)}, \tag{5a}$$

$$\dot{\gamma} = \sqrt{4\left(\frac{\partial u}{\partial z}\right)^2 - 4\frac{\partial v}{\partial r} \times \frac{v}{r} + \left(\frac{\partial u}{\partial r}+\frac{\partial v}{\partial z}\right)^2}. \tag{5b}$$

2.2 Numerical Solution

The solution of the flow problem in a converging pipe is possible using numerical techniques, since no analytical solution is developed for this problem, except approximate analytical solutions which are purposed for very slightly tapered (Bird et al., 1987) or converging (Hatzikiriakos and Mitsoulis, 2009) pipes. Therefore, the Galerkin finite element method (FEM) (Reddy and Gartling, 2010) is employed to calculate the pressure and the velocity components of the flow field, which is governed by viscous terms according to Eqs. 1a to 1c.

As shown in Fig. 1, rectangular elements can be fitted into the cross section of the converging pipe geometry. In each element bi-quadratic and bi-linear interpolation functions are assumed to calculate the velocity components and the pressure, respectively. Also, in order to have a better estimation for higher values of the strain rate near the wall, a finer mesh in that area has also been examined. In this regard, the value of α is defined as the width of the smallest element near the wall to that of the first one near the axis, as follows:

$$\alpha = \frac{w_i}{W_i} = \frac{w_o}{W_o}. \tag{6}$$

As shown in Fig. 1, w and W are the width of smallest and largest elements, respectively. Numbers of elements in radial (n_r) and axial (n_z) directions, as well as the value of α determine the meshing system in two dimensional flow problem in a converging pipe.

To consider the dependency of the viscosity on the strain rate, it is calculated at the center of each element according to Eq. 4. This leads to a non-linear set of equations, which is solved using direct substitution method. Also, to obtain a better converging solution, especially for highly shear thinning fluids (e. g. n = 0.4), the results of velocity components for a higher values of power-law index (e. g. n = 0.5) are employed as the first estimation.

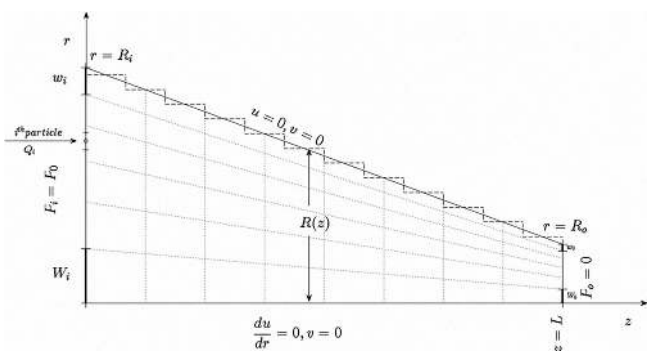

Fig. 1. The geometrical definitions, boundary condition and meshing system of converging pipe

2.3 Geometrical Parameters

The cross section of the converging pipe, as an axisymmetric geometry, is shown in Fig. 1. L is the pipe length, also R_i and R_o are the radius of the pipe at inlet and outlet, respectively. Moreover we define the converging ratio and the pipe dimensionless length by the dimensionless ratios of R_i/R_o and L/R_o, correspondingly.

2.4 Boundary Condition

A proper set of boundary conditions must be provided, to solve the differential equations of Eqs. 1a to 1c. In this regard, no slip boundary condition is set at the walls; therefore, as shown in Fig. 1 all of the velocity components are zero ($u = 0$ and $v = 0$) at $r = R(z)$. Also, based on the axisymmetric nature of the converging pipe, a relevant boundary condition is applicable on the axis, i. e. $\partial u/\partial r = 0$ and $v = 0$. Finally, as described in Shopov et al. (1994), a pressure inlet and pressure outlet boundary conditions are applied on the inlet and outlet of the converging pipe, respectively; as stated in Eqs. 7a and 7b:

$$-\tau_{nn|inlet} = P_i, \tag{7a}$$

$$-\tau_{nn|outlet} = 0, \tag{7b}$$

where n is a unit outward normal vector at the inlet and outlet of the converging pipe.

3 Mixing

3.1 Distributive Mixing

In the following, the mean strain function is calculated as the criterion for the distributive mixing. This can be accomplished by the particle trajectory method and evaluating the strain of each particles or fluid elements during its residence time in converging pipe (Cheng and Manas-Zloczower, 1998; Hanna-

chi and Mitsoulis, 1990). To achieve this objective, N mass less particles, which have no effect on the flow field (inert particle), are evenly distributed at the flow inlet and the path line of each particle is found out by integration of the velocity components over time, as stated in Eq. 8:

$$\begin{Bmatrix} r_i(t) \\ z_i(t) \end{Bmatrix} = \begin{Bmatrix} r_i(0) \\ z_i(0) \end{Bmatrix} + \int_0^t \begin{Bmatrix} v(r_i(t'), z_i(t')) \\ u(r_i(t'), z_i(t')) \end{Bmatrix} dt', = 1, \ldots, N. \tag{8}$$

In Eq. 8, $r_i(0)$ and $z_i(0)$, are the initial position of the i^{th} particle at the onset of the tracking; and, $r_i(t')$ and $z_i(t')$ are the positions of the i^{th} particle at time t'. When the i^{th} particle reaches to the outlet of the converging pipe ($z_i = L$), the upper limit of the integral will be its residence time ($t_{res,i}$). Therefore, the residence time of each particle can be estimated with Eq. 9:

$$\begin{Bmatrix} r_i(t) \\ L \end{Bmatrix} = \begin{Bmatrix} r_i(0) \\ 0 \end{Bmatrix} + \int_0^{t_{res,i}} \begin{Bmatrix} v(r_i(t'), z_i(t')) \\ u(r_i(t'), z_i(t')) \end{Bmatrix} dt', = 1, \ldots, N. \tag{9}$$

According to Eq. 9, it is expected to have N different residence times for each N inert particle. By a weighted average of the residence times, the mean residence time is calculated as follows:

$$\bar{t} = \int_0^\infty t'' f(t'') dt''. \tag{10}$$

In Eq. 10, the weight function of $f(t'')$ is the portion of the flow that have a residence time in the range of $t'' - dt''/2$ to $t'' + dt''/2$. To evaluate Eq. 10 numerically, we consider Q_i being the flow rate in the vicinity of the i^{th} inert particle, which have a residence time in the range of $\left[\frac{t_{res,i-1} + t_{res,i}}{2} \; \frac{t_{res,i} + t_{res,i+1}}{2}\right]$. Consequently, the portion of the flow (f_i), which has the average residence time of $t_{res,i}$ is calculated by Eq. 11:

$$f_i = \frac{Q_i}{Q}, \tag{11}$$

where Q is the total flow rate of the converging pipe $\left(\sum_{i=1}^{N} Q_i\right)$. Therefore, the mean residence time, which is defined in Eq. 9, is estimated with Eq. 12:

$$\bar{t} = \sum_{i=1}^{N} f_i \times t_{res,i}, \tag{12}$$

$\bar{t}$ in Eq. 12 is the mean residence time which is calculated using the results of particle trajectory method; nevertheless, the mean residence time can be estimated by Eq. 13 (Gogos and Tadmor, 1979; Hannachi and Mitsoulis, 1990), which is independent of the particle residence times.

$$t_m = \frac{\text{Pipe volume}}{Q}, \tag{13}$$

t_m in Eq. 13 is another expression for the mean residence time and must be equal to $\bar{t}$.

In a similar way, the mean strain function ($\bar{\gamma}$) (Bigg and Middleman 1974, Gogos and Tadmor 1979), which is defined in Eq. 14,

$$\bar{\gamma} = \sum \int_0^\infty \gamma'' f(t'') dt'', \tag{14}$$

can be evaluated as follows:

$$\bar{\gamma} = \sum_{i=1}^{N} f_i \times \gamma_i. \tag{15}$$

In Eq. 14, γ'' is the total strain of the flow portion with the residence time in the range of $t'' - dt''/2$ to $t'' + dt''/2$. Correspondingly, in Eq. 15, γ_i is the total strain of the i^{th} particle, which is calculated as follows:

$$\gamma_i = \int_o^{t_{res,i}} \dot{\gamma}(r_i(t'), z_i(t')) dt'. \tag{16}$$

The strain rate in the Eq. 16 is calculated according to Eq. 5. In other word, both elongation and shear strain rates are considered in calculation of the mean strain function.

In Eq. 16, the size of the time step (dt') must be small enough to guarantee that the total strain (γ_i) is independent of the time increment; and this procedure must be repeated for all of the inert particles (N) which are introduced in to the converging pipe. Considering the fact that the accuracy of Eqs. 12 and 15 depend on N, we can conclude that these calculations are time consuming tasks, and the CPU time depends on N and the time increment. So the number of the inert particles must be chosen in a way that provides us exact but not very costly results. In this research, the number of particle is chosen according to the smallest nodal space at the pipe inlet, as follow:

$$N = \text{integer}\left(\frac{4R_i}{w_i}\right) \leq \frac{4R_i}{w_i}. \tag{17}$$

3.2 Dispersive Mixing

It is believed that the dispersive mixing benefits elongation flow fields more than shear flows. This is attributed to the non-zero component in vorticity tensor of the shear flow, which leads to solid rotation of agglomerates and droplets (Connelly and Kokini, 2004; Manas-Zloczower, 2012; Yao and Manas-Zloczower, 1996).

Since the flow field in a converging pipe comprises elongational strain rates, dispersive mixing has also been studied in this research. For this purpose we have employed the Manas-Zloczower mixing index λ (Cheng and Manas-Zloczower, 1997; Wang and Manas-Zloczower, 2001; Yao and Manas-Zloczower, 1996), which is introduced in Eq. 18:

$$\lambda = \frac{\dot{\gamma}}{\dot{\gamma} + \omega}. \tag{18}$$

Here ω is the magnitude of the vorticity tensor, which is defined in Eqs. 19a and 19b:

$$\bar{\bar{\omega}} = \begin{pmatrix} 0 & \frac{\partial v}{\partial z} - \frac{\partial u}{\partial r} \\ \frac{\partial u}{\partial r} - \frac{\partial v}{\partial z} & 0 \end{pmatrix}, \tag{19a}$$

$$\omega = \sqrt{\frac{1}{2}\, \bar{\bar{\omega}} : \bar{\bar{\omega}}}. \tag{19b}$$

As stated in Eq. 20, a volume weighted average of the Manas-Zloczower mixing index in the domain, $\bar{\lambda}$, is defined as follows:

$$\bar{\lambda} = \frac{\Sigma \lambda_i V_i}{\Sigma V_i}. \tag{20}$$

In Eq. 20, λ_i and V_i are the dispersive mixing index and the volume of each element, and the summation is performed over all of the elements.

4 Verification and Mesh Independency

As it was described in section 3.1, the accuracy of the mean strain function depends on the number of inert particles as well as the time increment in Eq. 15. In an appropriate meshing system, in which the number of the inert particles is defined by Eq. 17, the value of the mean strain function must be mesh-independent.

To find a suitable meshing system, the results of the mean strain function and the mean residence time are compared with their analytical values, for the case of the parallel pipe for which analytical solution is available, as stated in Eqs. 21a to 21c (Gogos and Tadmor, 1979):

$$\bar{\gamma}_a = 2\frac{L}{\bar{R}}\frac{3n+1}{2n+1} \tag{21a}$$

$$\bar{R} = \sqrt{\frac{R_o^2 + R_i R_o + R_i^2}{3}}, \tag{21b}$$

$$\bar{t}_a = \frac{L}{\bar{U}}. \tag{21c}$$

In Eq. 21a, the term $\bar{\gamma}_a$ is the analytical value of the mean strain function and $\bar{R}$, as defined in Eq. 21b, is the radius of a parallel pipe with the same volume as the converging pipe. The value of $\bar{R}$ is equal to the inlet and outlet radius, for the case of a parallel pipe. $\bar{t}_a$ and $\bar{U}$ in Eq. 21c are the analytical values of the mean residence time and the mean velocity.

Figure 2 illustrates the values of $\bar{\gamma}$ and $\bar{t}$, which are normalized by analytical values of $\bar{\gamma}_a$ and $\bar{t}_a$, respectively, versus mesh number of in the radial direction (n_r). It shall be noted that the mesh number in the axis direction (n_z) is chosen to be $2 \times n_r$.

Moreover Fig. 2 shows that by increasing n_r the normalized values of $(\bar{\gamma}/\bar{\gamma}_a)$ and $(\bar{t}/\bar{t}_a)$ approach toward unity; in other word, the values of the mean strain function and the mean residence time become independent of the meshing system. Also, it can be inferred that for some meshing systems (α = 1/5 and 1/10 after n_r = 30 the results are mesh-independent.

For a converging pipe for which no exact analytical solution is provided, the comparison of the residence times, which are derived from Eqs. 12 and 13 as two completely different approaches ($\bar{t}$ and t_m), is used to prove the mesh independency and the validity of the results. Figure 3A shows the dimensionless ratio of $\bar{t}/\bar{t}_m$ for different meshing systems, where t_m is calculated by the results of similar simulation in OpenFOAM (Technische Universität Dresden, Dresden, Germany).

In Fig. 3A it can be observed that by increasing the mesh number, the ratio of $\bar{t}/\bar{t}_m$ inclines toward unity; and after n_r = 30 for some meshing systems becomes independent of the meshing system. A comparison of the mean residence times for tapered pipes with different converging ratios and lengths for variety of rheological behavior (power-law index) is also presented in Fig. 3B, as typical results. The good conformity between the in-house software and OpenFOAM results; reveals the fact that the numerical calculations in this research are reliable and mesh independent. Similarly, the area weighted average of the distributive mixing index ($\bar{\lambda}$) is examined to be mesh independent, which is omitted here for conciseness.

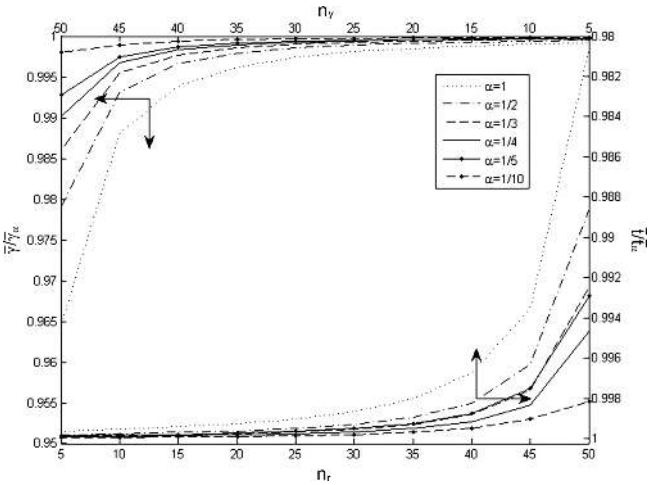

Fig. 2. Normalized values of the mean strain function ($\bar{\gamma}/\bar{\gamma}_a$) and the mean residence time ($\bar{t}/\bar{t}_a$), for different meshing system

According to Fig. 2 and 3, it can be inferred that mesh independent results can be obtained by n_r = 30; however, in our simulation n_r is set to be 40. Therefore, the number of elements and nods are 3 200 and 13 041, respectively. Also, according to the bi-quadratic and bi-linear shape functions, which are chosen for the calculation of the velocity components and the pressure in each element, the degree of freedom will be 29 403. The simulations are performed on an Intel Xeon CPU E5-2640 0 (Technische Universität Dresden, Dresden, Germany) at 2.50 GHz, 2.49 GHz and installed RAM of 29.2 GB using the software MATLAB 8.3.0.532 R2014a (Technische Universität Dresden, Dresden, Germany).

5 Approximate Expression for Distributive Mixing

As described in section 3.1, the evaluation of the mean strain function using numerical method is a time consuming task; therefore, it would be useful to express it analytically. Because of the nonzero components of the strain rate tensor, no exact analytical solution can be considered for the flow problem in a converging pipe (Bird et al., 1987; Hatzikiriakos and Mitsoulis, 2009); and thus also not for the mean strain function, as a matter of fact. Nevertheless, in this research, an approximate analytical expression for the mean strain function is developed, using the following three simplifying assumptions.

By considering $\bar{U}(z)$ as the average velocity in each cross section of the pipe with the radius of r(z), the normal strain rates ($\dot{\gamma}_{zz}$), as the first assumption, can be estimated as follows (Gogos and Tadmor, 1979):

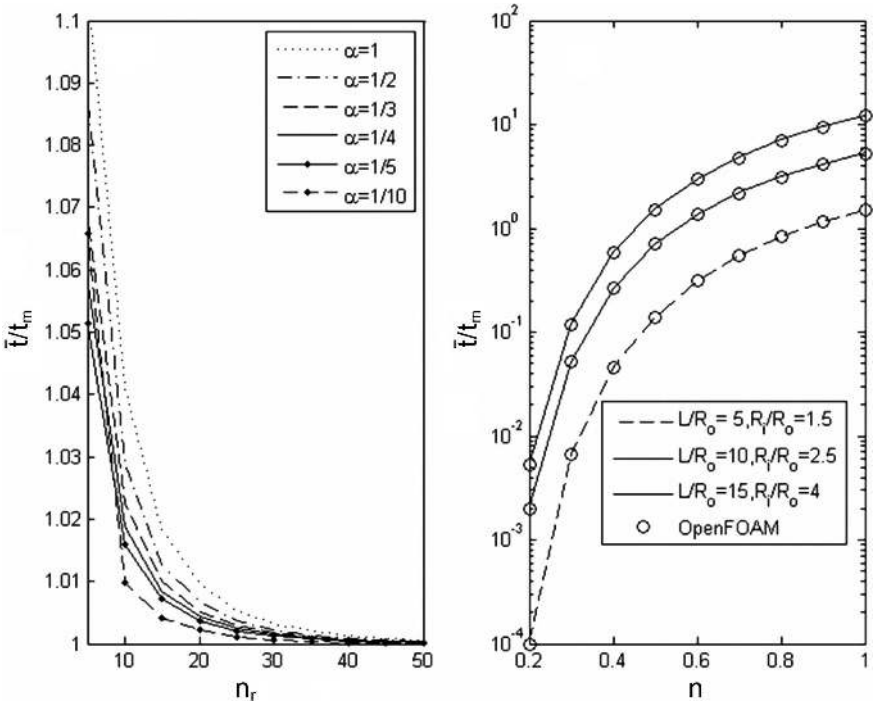

A) B)

Fig. 3. Comparison of the mean residence times, which are calculated based on Eqs. 12 (t) and 13 (t_m), using the in-house software and OpenFOAM, respectively, (A) the results of different meshing systems for a tapered pipe with $R_i/R_o = 2.5$, $L/R_o = 10$, and $n = 0.6$, (B) the results of residence time for tapered pipes with different rheological and geometrical parameters

$$|\dot{\gamma}_{rr} + \dot{\gamma}_{\theta\theta}| = |\dot{\gamma}_{zz}| = 2\left|\frac{\partial u}{\partial z}\right| \approx 2\left|\frac{\partial \bar{U}(z)}{\partial z}\right|. \tag{22}$$

The term $\bar{U}(z)$ in Eq. 22, is calculated by Eqs. 23a and 23b:

$$\bar{U}(z) = \frac{Q}{\pi \times R(z)^2}, \tag{23a}$$

$$R(z) = R_i - \frac{R_i - R_o}{L} \times z. \tag{23b}$$

By replacing Eqs. 23a and 23b in Eq. 22, the magnitude of the normal strain rates is calculated as stated in Eq. 24:

$$|\dot{\gamma}_{rr} + \dot{\gamma}_{\theta\theta}| = |\dot{\gamma}_{zz}| = 4\frac{R_i - R_o}{L} \times \frac{\bar{U}(z)}{R(z)}. \tag{24}$$

It is believed that the velocity profile in each cross section of a slightly converging pipe can be approximated by that of a parallel pipe with the same diameter (Bird et al., 1987). In other words, the converging pipe can be assumed to be composed of an infinite number of imaginary parallel pipes with different diameters, as shown in Fig. 1. In place of the second assumption, this idea is extended to all of the converging ratios; therefore, the shear strain rate in each cross section is estimated as follows:

$$|\dot{\gamma}_{rz}| = |\dot{\gamma}_{zr}| = \left|\frac{\partial u}{\partial r} + \frac{\partial v}{\partial z}\right| \approx \left|\frac{\partial u}{\partial r}\right| = \frac{3n+1}{n} \times \frac{\bar{U}(z)}{R(z)} \times \left(\frac{r}{R(z)}\right)^{\frac{1}{n}}. \tag{25}$$

Based on the first and second assumption, the magnitude of the strain rate tensor in Eq. 5, can be simplified as follow:

$$\dot{\gamma} = \sqrt{\left(\frac{\partial u}{\partial r}\right)^2 + 4\left(\frac{\partial u}{\partial z}\right)^2}. \tag{26}$$

This equation can be reformed into Eqs. 27a and 27b:

$$\dot{\gamma} = \dot{\gamma}_a \sqrt{1 - 4\frac{\left|\frac{\partial u}{\partial r}\right|}{\dot{\gamma}_a}\frac{\left|\frac{\partial u}{\partial z}\right|}{\dot{\gamma}_a}}, \tag{27a}$$

$$\dot{\gamma}_a = \left|\frac{\partial u}{\partial r}\right| + 2\left|\frac{\partial u}{\partial z}\right|, \tag{27b}$$

According to the second assumption for each imaginary parallel pipe, the term $\left|\frac{\partial u}{\partial z}\right|/\dot{\gamma}_a$ is zero on the walls due to the no slip boundary condition. Moreover, the term $\left|\frac{\partial u}{\partial r}\right|/\dot{\gamma}_a$ is zero on the axis, where a symmetric boundary condition is applied. Therefore, the product of $\left|\frac{\partial u}{\partial z}\right|/\dot{\gamma}_a$ and $\left|\frac{\partial u}{\partial r}\right|/\dot{\gamma}_a$ is ignorable in the area nearby the wall areas and the axis. As the third assumption, the expression of $\left|\frac{\partial u}{\partial r}\right|\left|\frac{\partial u}{\partial z}\right|$ is considered to be ignorable in comparison with $\dot{\gamma}_a^2$ in the whole domain; so, the magnitude of the strain rate tensor is simplified as given in Eq. 28:

$$\dot{\gamma} \approx \dot{\gamma}_a. \tag{28}$$

The term $\dot{\gamma}_a$ in Eq. 28 overestimates the magnitude of the strain rate tensor; but still approaches toward the exact value as the ratio of $(R_i - R_o)/L$ tends toward zero ($R_i \to R_o$ or $L \to \infty$).

Nevertheless, using this simplified expression, the mean strain function in each cross section of the converging pipe can be calculated, as follows:

$$d\gamma = \frac{dz}{R(z)}\left(\frac{3n+1}{2n+1} + 2\frac{R_i - R_o}{L}\right). \quad (29)$$

The approximate expression of the mean strain function is calculated by integrating Eq. 29 along the length of the pipe, which is stated in Eq. 30:

$$\gamma = 2\left(\frac{3n+1}{2n+1} + 2\frac{R_i - R_o}{L}\right) \times \frac{\ln\left(\frac{R_i}{R_o}\right)}{\frac{R_i - R_o}{L}}. \quad (30)$$

In a slightly converging pipe, where the magnitude of $(R_i - R_o)/L$ is very small ($R_i \to R_o$ or $L \to \infty$), Eq. 30 approaches toward the mean strain function of a parallel pipe, which is stated in Eq. 21a. Nevertheless, as the term $(R_i - R_o)/L$ increases, Eq. 30 deviates more from the exact values of the mean strain function. Therefore, Eq. 31 is defined by introducing the coefficient β_1 and the exponents β_2 and β_3 to Eq. 30 to improve its conformity with the numerical results.

$$\gamma = 2\beta_1\left(\frac{3n+1}{2n+1} + 2\frac{R_i - R_o}{L}\right)^{\beta_2} \times \left(\frac{\ln\left(\frac{R_i}{R_o}\right)}{\frac{R_i - R_o}{L}}\right)^{\beta_3}. \quad (31)$$

Using the numerical values of the mean strain function ($\gamma = \bar{\gamma}$), the parameters β_1, β_2 and β_3 can be evaluated with linear regression technique. The result of the calculations shows that the parameters of β_1 and β_3 have the value of unity, independent of the geometrical $\left(\frac{R_i}{R_o} \text{and} \frac{L}{R_o}\right)$ and rheological (n) parameters; and the exponent β_2, which is also independent of the power-law index, can be described by Eq. 32:

$$\beta_2 = 1 - \frac{2}{5}\left(\exp\left(\left(\left(\frac{0.2}{\left(\frac{L}{R_0}\right)^{1/\left(\frac{1}{R_o}\right)}} - 0.2\right) \times \left(\frac{R_i}{R_o} - 1\right)\right)\right.$$

$$\left. - \exp\left(\frac{14}{\left(\frac{L}{R_0}\right)} \times \left(1 - \frac{R_i}{R_o}\right)\right)\right). \quad (32)$$

It is obvious from Eq. 32 the exponent β_2 approaches unity as the term $(R_i - R_o)/L$ becomes smaller, which is the case of a slightly converging pipe.

6 Results and Discussion

Since the quality of the dispersive and distributive mixing is affected by the operating condition and the geometrical design of the mixing device as well as by the rheological behavior of the mixture, the effects of different operational, geometrical and rheological parameters on the dispersive and distributive mixing were studied. In order to cover a wide range of parameters, the converging ratio, pipe dimensionless length and power-law index were chosen to be in the ranges of [1 to 4], [5 to 15] and [0.2 to 1.0], respectively.

By increasing the pressure difference between the inlet and outlet of the pipe ($P_i - P_o$), as an operating condition, the velocity components (u, v), the components of strain rate tensor ($\bar{\dot{\gamma}}$) and vorticity tensor ($\bar{\omega}$) will subject to growth, as well. But, the residence time ($\bar{t}$) drops proportionally. Therefore, the distributive mixing parameter (γ), as product of the strain rate and the residence time, and the dispersive mixing index ($\bar{\lambda}$), which is defined by the ratio of rate and vorticity tensors, will both remain unchanged.

Figure 4 shows the cumulative residence time distribution function F(t) for different power-law indexes, converging rations and pipe lengths. The cumulative residence time or F(t) is the portion of the inlet (or outlet) flow, which has residence time less than t (Gogos and Tadmor, 1979).

In Fig. 4, the assessment of the straight pipe and the tapered pipe with n = 0.2 reveals that by decreasing of the converging ratio the residence time distribution curve tends toward that of plug flow, in which no distributive mixing can be considered. So, an increase of the converging ratio can improve the distributive mixing. The effect of the converging ratio on the residence time can also be observed by evaluation of the other cases ($L/R_o = 5$, $n = 0.6$) with different converging ratios ($R_i/R_o = 4,2$). In a similar way, it can be expected that by increasing the pipe length ($L/R_o = 5$ to 10) for the cases with similar converging ratio and power-law index ($R_i/R_o = 4$, $n = 0.6$), a narrower residence time distribution and consequently a weaker distributive mixing will be obtained. Moreover, the comparison of similar converging pipes ($R_i/R_o = 4$, $L/R_o = 5$) with different rheological behavior of the fluid (n = 0.2, 0.6 ansd 1) shows that, a decrease in shear thinning behavior provides a wider residence time distribution and a better distributive mixing, as a result.

To clarify the dependency of the distributive mixing on the rheological behavior (n), the relation of the mean strain function and the power-law index is studied in Fig. 5A. The figure

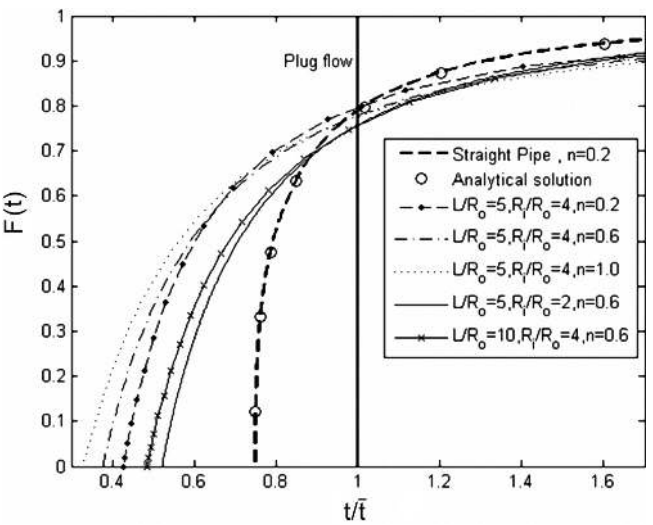

Fig. 4. Comparison of the cumulative residence time for a tapered pipe with different rheological and geometrical parameters

shows that the rise of the power-law index is accompanied by a growth for the mean strain function. This can be correlated to the wider residence time distribution which is observed in Fig. 4 for a Newtonian fluid. Similar trend is also observed by Bigg and Middleman (1974) for single screw extruder. In this figure, the analytical values of the mean strain function are also presented by marked lines. The good conformity between the analytical and the numerical results reveals the capability of the approximate expression in the evaluation of the mean strain function.

In Fig. 5B the dependency of the dispersive mixing, which is evaluated by the Manas-Zloczower mixing index, on the power-law index is shown. It can be observed that, in spite of the distributive mixing, the parameter of $\bar{\lambda}$ drops as n approaches to unity. In other words, the dispersive mixing benefits from shear thinning behavior; nevertheless, this is not the case for the distributive mixing.

Figure 6A and 6B demonstrate the effect of the converging ratio on the normalized mean strain function and dispersive mixing index. Figure 6A reveals that by increasing the converging ratio the normalized mean strain function increases accordingly. This is attributed to the development of normal strain rates which do not exist in straight pipes. This is what was expected from Fig. 4, in which wider residence time distributions were presented for the pipes with greater converging ratios. This graph also shows a good conformity between the numerical and the analytical values, which are presented by the marked lines.

Normal strain rates not only improve the distributive mixing, but also enhance the dispersive mixing ($\bar{\lambda}$). In Fig. 6B, it is observed that for $R_i/R_o = 1$ the parameter of $\bar{\lambda}$ is 1/2, as a characteristic of pure shear flows (Yao and Manas-Zloczower 1996); then by increasing the converging ratio it will be subjected to a growth as well, especially for highly shear thinning fluids.

Figure 7 shows the effect of the dimensionless length (L/R_o) on the distributive and dispersive mixing. In Fig. 7A the growth of the mean strain function with L/R_o is presented. This is attributed to the longer residence time of the inert particle or fluid element inside the converging pipe, which is thus subject to more deformations. In this graph the analytic results (marked lines) comply with the numerical results, as it was the case in Figs. 5A and 6A.

By increasing L/R_o, the term $(R_i - R_o)/L$ becomes smaller, as well as the normal strain rates. Therefore, it is expected to have lower values of the dispersive mixing as the dimensionless length increases. This trend is illustrated in Fig. 7B. Also, the comparison of the similar converging pipes, with n = 0.2 and n = 0.6, shows that by an increase of the shear thinning behavior, the dispersive mixing index will be less affected by the length of the pipe.

7 Conclusion

Different aspects of laminar mixing, as an important step in polymer processing, have been studied in a converging pipe. For this purpose the flow field components have been calculated by a new developed finite element code. Then, using the particle trajectory method, the mean strain function as a criterion for distributive mixing is evaluated. Also, to assess the dispersive mixing, the Manas-Zloczower mixing index has been chosen; which is calculated using the strain rate and vorticity tensor in each element.

It has been stated that dispersive and as well as distributive mixings are independent of the flowrate or the pressure difference of the pipe; but, are affected by the pipe length, converging ratio and power-law index. This complex dependency was shown using a parametric study based on the results ob-

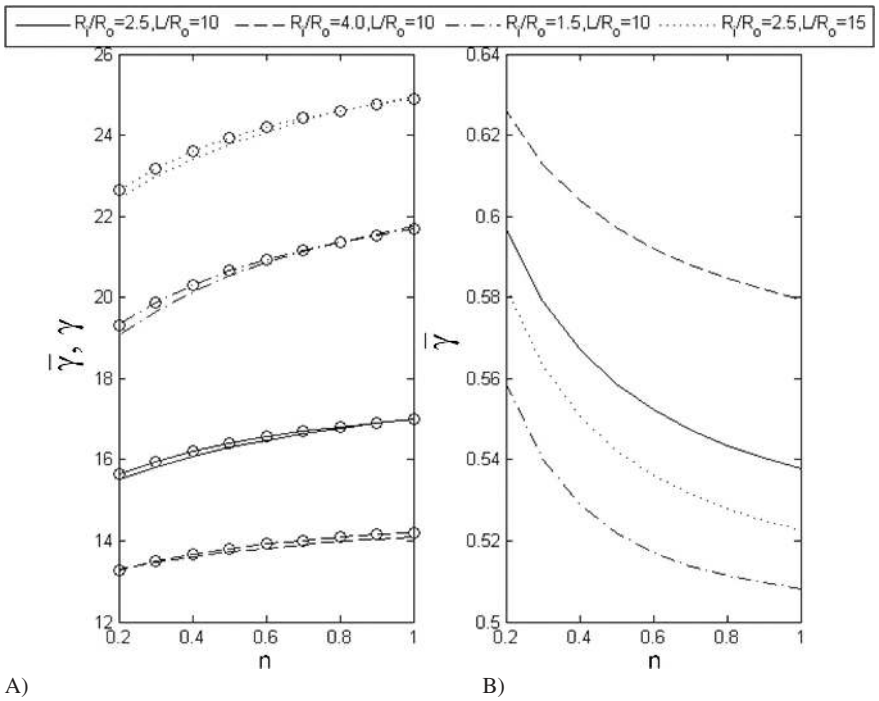

Fig. 5. The effect of the power-law index on the distributive and dispersive mixing, (A) effect of n on the mean strain function. Marked lines are results of the analytical expression. (B) effect of n on $\bar{\lambda}$

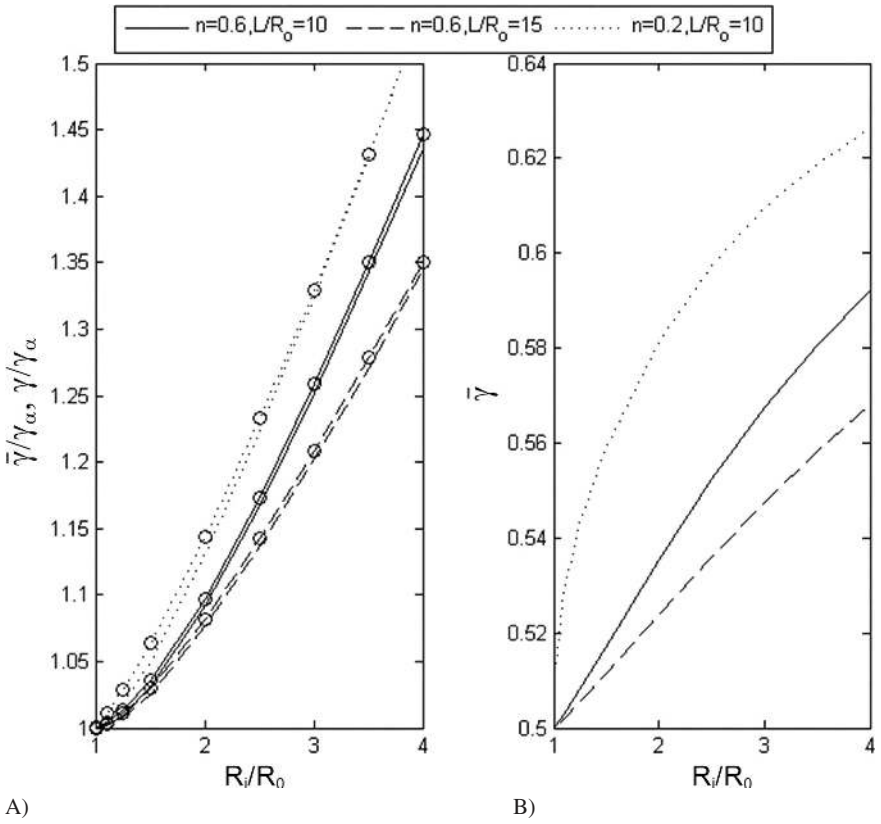

A) B)

Fig. 6. The effect of the converging ratio index on the distributive and dispersive mixing, (A) effect of the converging ratio on the mean strain function. Marked lines are results of the analytical expression. (B) effect of the converging ratio on $\bar{\lambda}$

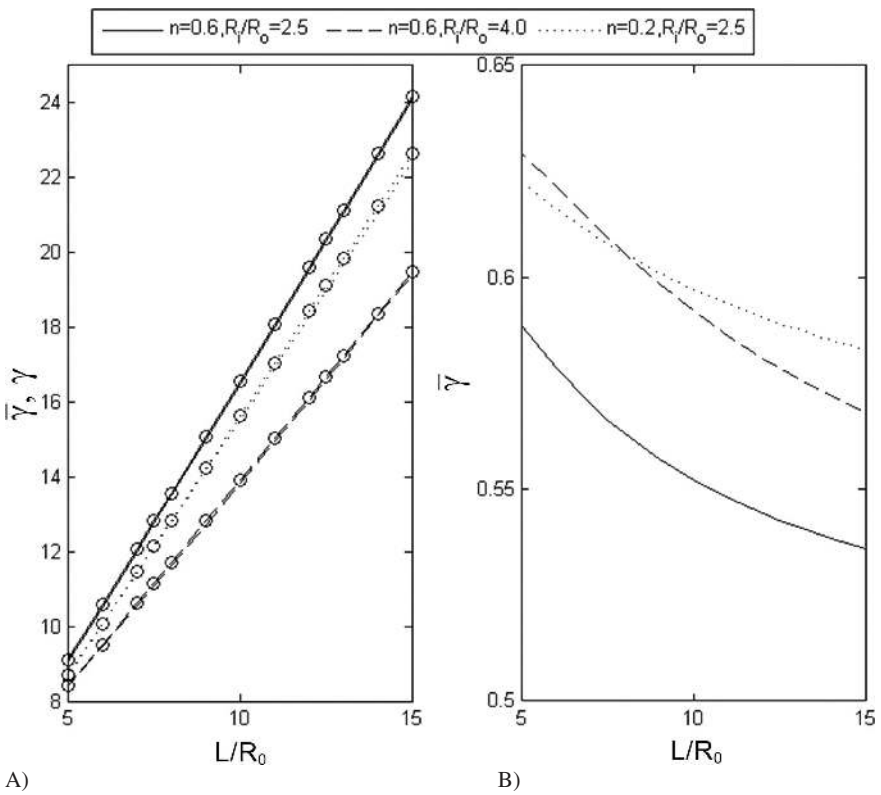

A) B)

Fig. 7. The effect of the dimensionless length on the distributive and dispersive mixing, (A) effect of the dimensionless length on the mean strain function. Marked lines are results of the analytical expression. (B) effect of the dimensionless length on $\bar{\lambda}$

tained from numerical calculations; however, an analytical approximate expression for the distributive mixing has been derived, by employing three simplifying assumptions and curve fitting technique, which can satisfactorily evaluate the mean strain function in a much shorter computation time in comparison with the numerical solution.

References

Alemaskin, K., Manas-Zloczower, I. and Kaufman, M., "Color Mixing in the Metering Zone of a Single Screw Extruder: Numerical Simulations and Experimental Validation", Polym. Eng. Sci., **45**, 1011–1020 (2005), DOI:10.1002/pen.20368

Ausias, G., Jarrin, J. and Vincent, M., "Optimization of the Tube-Extrusion Die for Short-Fiber-Filled Polymers", Compos. Sci. Technol., **56**, 719–724 (1996), DOI:10.1016/0266-3538(96)00012-7

Bigg, D., Middleman, S., "Mixing in a Screw Extruder. A Model for Residence Time Distribution and Strain", Ind. Eng. Chem. Fundam., **13**, 66–71 (1974), DOI:10.1021/i160049a013

Bigio, D. I., Boyd, J. D., Erwin, L. and Gailus, D. W., "Mixing Studies in the Single Screw Extruder", Polym. Eng. Sci., **25**, 305–310 (1985), DOI:10.1002/pen.760250510

Bigio, D., Zerafati, S., "Parametric Study of a 2-D Model of the Nip Region in a Counter-Rotating, Non-Intermeshing Twin Screw Extruder", Polym. Eng. Sci., **31**, 1400–1410 (1991), DOI:10.1002/pen.760311906

Bird, R. B., Armstrong, R. C. and Hassager, O.: Dynamics of Polymeric Liquids. Fluid Mechanics, Volume 1, Wiley-Interscience Publication, John Wiley & Sons, New York (1987)

Cheng, H., Manas-Zloczower, I., "Study of Mixing Efficiency in Kneading Discs of Co-Rotating Twin-Screw Extruders", Polym. Eng. Sci., **37**, 1082–1090 (1997), DOI:10.1002/pen.11753

Cheng, H., Manas-Zloczower, I., "Distributive Mixing in Conveying Elements of a ZSK-53 Co-Rotating Twin Screw Extruder", Polym. Eng. Sci., **38**, 926–935 (1998), DOI:10.1002/pen.10260

Connelly, R. K., Kokini, J. L., "The Effect of Shear Thinning and Differential Viscoelasticity on Mixing in a Model 2D Mixer as Determined Using FEM with Particle Tracking", J. Non-Newtonian Fluid Mech., **123**, 1–17 (2004), DOI:10.1016/j.jnnfm.2004.03.006

Erwin, L., Mokhtarian, F., "Analysis of Mixing in Modified Single Screw Extruders", Polym. Eng. Sci., **23**, 49–60 (1983), DOI:10.1002/pen.760230202

Fard, A. S., Famili, N. M. and Anderson, P. D., "A New Adaptation of Mapping Method to Study Mixing of Multiphase Flows in Mixers with Complex Geometries", Comput. Chem. Eng., **32**, 1471–1481 (2008), DOI:10.1016/j.compchemeng.2007.06.023

Funt, J.: Mixing of Rubber, RAPRRA Publication, Shawbury, UK (1977)

Galaktionov, O. S., Anderson, P. D., Peters, G. W. M. and Tucker, C. L. , "A Global, Multi-Scale Simulation of Laminar Fluid Mixing: The Extended Mapping Method", Int. J. Multiphase Flow, **28**, 497–523 (2002), DOI:10.1016/S0301-9322(01)00080-5

Gale, M., "Compounding with Single-Screw Extruders", Adv. Polym. Technol., **16**, 251–262 (1997), DOI:10.1002/(SICI)1098-2329(199711)16:4<251::AID-ADV1>3.0.CO;2-U

Gogos, C. G., Tadmor, Z.: Principles of Polymer Processing, Wiley-Interscience Publication, John Wiley & Sons, Dunfermline (1979)

Hannachi, A., Mitsoulis, E., "Deformation Fields and Residence Time Distributions in Polymer Melt Flows", Int. Polym. Proc, **5**, 244–251 (1990), DOI:10.3139/217.900244

Hatzikiriakos, S. G., Mitsoulis, E., "Slip Effects in Tapered Dies", Polym. Eng. Sci., **49**, 1960–1969 (2009), DOI:10.1002/pen.21430

Kalyon, D. M., Sangani, H. N., "An Experimental Study of Distributive Mixing in Fully Intermeshing, Co-Rotating Twin Screw Extruders", Polym. Eng. Sci., **29**, 1018–1026 (1989), DOI:10.1002/pen.760291508

Kwon, T., Joo, J. and Kim, S., "Kinematics and Deformation Characteristics as a Mixing Measure in the Screw Extrusion Process", Polym. Eng. Sci., **34**, 174–189 (1994), DOI:10.1002/pen.760340303

Li, T., Manas-Zloczower, I., "A Study of Distributive Mixing in Counterrotating Twin Screw Extruders", Int. Polym. Proc., **10**, 314–320 (1995), DOI:10.3139/217.950314

Maheshri, J. C., Wyman, C. E., "Mixing in an Intermeshing Twin Screw Extruder Chamber: Combined Cross and Down Channel Flow", Polym. Eng. Sci., **20**, 601–607 (1980), DOI:10.1002/pen.760200904

Manas-Zloczower, I.: Mixing and Compounding of Polymers: Theory and Practice, Hanser, Munich (2012)

Mostafaiyan, M., Saeb, M. R., Ahmadi, Z., Khonakdar, H. A., Wagenknecht, U. and Heinrich, G., "A Numerical Study on Deformation of Newtonian Droplets through Converging Cylindrical Dies", E-Polymers, **13**, 49–66 (2013), DOI:10.1515/epoly-2013-0106

Mostafaiyan, M., Wiessner, S. and Heinrich, G., "The Study of the Distributive Mixing in Converging Channels: Numerical Method and Analytical Approach", Polym. Eng. Sci., **55**, 2285–2292 (2015)

Reddy, J. N., Gartling, D. K.: The Finite Element Method in Heat Transfer and Fluid Dynamics, CRC Press, London (2010)

Shopov, P. J., Iordanov, Y. I., "Numerical Solution of Stokes Equations with Pressure and Filtration Boundary Conditions", J. Comput. Phys., **112**, 12–23 (1994), DOI:10.1006/jcph.1994.1078

Tokihisa, M., Yakemoto, K., Sakai, T., Utracki, L. A., Sepehr, M., Li, J. and Simard, Y., "Extensional Flow Mixer for Polymer Nanocomposites", Polym. Eng. Sci., **46**, 1040–1050 (2006), DOI:10.1002/pen.20542

Wang, W., Manas-Zloczower, I., "Temporal Distributions: The Basis for the Development of Mixing Indexes for Scale-Up of Polymer Processing Equipment", Polym. Eng. Sci., **41**, 1068–1077 (2001), DOI:10.1002/pen.10807

Wang, W., Manas-Zloczower, I. and Kaufman, M., "Entropic Characterization of Distributive Mixing in Polymer Processing Equipment", AIChE J., **49**, 1637–1644 (2003), DOI:10.1002/aic.690490704

Wong, T. H., Manas-Zloczower, I., "Two-Dimensional Dynamic Study of the Distributive Mixing in an Internal Mixer", Int. Polym. Proc., **9**, 3–10 (1994), DOI:10.3139/217.940003

Yao, C. H., Manas-Zloczower, I., "Study of Mixing Efficiency in Roll-Mills", Polym. Eng. Sci., **36**, 305–310 (1996), DOI:10.1002/pen.10417

Zhou, D., Yue, P. and Feng, J. J., "Viscoelastic Effects on Drop Deformation in a Converging Pipe Flow", J. Rheol., **52**, 469–487 (2008), DOI:10.1122/1.2837525

Date received: October 01, 2015
Date accepted: February 06, 2016

Bibliography
DOI 10.3139/217.3179
Intern. Polymer Processing
XXXI (2016) 3; page 327–335

ISSN 0930-777X